Characterization of a model Ziegler–Natta catalyst for ethylene polymerization

J. Schmidt, T. Risse,[a] H. Hamann, and H.-J. Freund
Fritz-Haber-Institut der Max-Planck-Gesellschaft, Faradayweg 4-6, D-14195 Berlin, Germany

(Received 8 January 2002; accepted 28 March 2002)

Based on the work of the Somorjai group [Magni and Somorjai, Catal. Lett. **35**, 205 (1995)] we have prepared a thin well ordered $MgCl_2(001)$ film by $MgCl_2$ evaporation from a Knudsen cell. This film does not absorb $TiCl_4$ at room temperature if it is not activated by increasing the defect density via electron or ion bombardment. The nature of some of the defects created is characterized by *in situ* ESR measurements and Auger spectroscopy. Paramagnetic surface defects are altered by the bonding of $TiCl_4$ to the surface as observed by ESR spectroscopy. Ti^{3+} centers are detected if particularly severely defected $MgCl_2$ layers are prepared. Reactivity studies show however, that these species are not correlated with polymerization activity. Interaction with aluminum alkyl leads to the formation of the active catalyst and we observe for the first time directly ethyl radicals formed from trimethyl-aluminum in an abstraction process which may be formulated as $TiCl_4/^{surface} + AlMe_3 \rightarrow Me-TiCl_3/^{surface} + AlMe_2Cl$, $Me-TiCl_3/^{surface} \rightarrow TiCl_3/^{surface} + Me\cdot$, and $Me\cdot + Me_3Al \rightarrow C_2H_5\cdot + AlH(Me)_2$. The presence of the aluminum alkyl is observed via *in situ* IRAS in the same apparatus. © *2002 American Institute of Physics.* [DOI: 10.1063/1.1479722]

I. INTRODUCTION

Transition metal (in particular titanium) halides and organoaluminum compounds have been in use since Ziegler's early work in the early 1950's[2] to (homogeneously) catalyze the polymerization of ethylene.[3,4] Together with the extension of Ziegler's work by Natta[5] to use these systems in the synthesis of stereo regular poly(α)alkenes, the basis for more than 10% of all profits made with organometallic catalysts have been laid.[6] Since the development of the first generation Ziegler–Natta catalysts, several generations of such catalysts have been put in place which exhibit orders of magnitude, higher activity, and efficiency.[4] The third generation of Ziegler–Natta catalysts actually represents a supported catalyst which has been developed and used since 1975 in order to increase the amount of active Ti using inorganic chlorides, such as $MgCl_2$ and $CoCl_2$ as supports.[7] The high activity of these catalysts allowed use of low catalyst concentrations and, therefore, catalyst residues can remain in the polymer.[4] The literature on the topic of Ziegler–Natta catalysis is huge[4,6,8] and still growing since the development of the new generation of metallocenes/methylaluminoxane catalysts has recently increased interest in this field substantially.[3,9] There are several excellent reviews on the subject[4,6,8] and we would like to refer to one by Kaminski and Arndt,[4] in particular.

Interesting and important contributions to our understanding have recently been gained through theoretical studies by Parrinello and his group (see, e.g. Ref. 10).

The experimental characterization of supported third generation Ziegler–Natta catalysts has been mainly indirectly done in the past via polymer product analysis. However, as has been frequently stated in the literature,[4,6,8] knowledge on surface properties of such systems is of fundamental importance to describe the process and its mechanism in detail. Surface science studies on polymerization catalysts have been rather scarce. Model studies on the Phillips catalyst have been performed[11] and most importantly for the present paper, Somorjai and co-workers[1,12,13] published a series of publications on the preparation and characterization of model systems for supported Ziegler–Natta catalysts. These model systems have been used to polymerize ethylene.

The model consists of an epitaxially grown $MgCl_2$ film onto which $TiCl_4$ is anchored, followed by the so-called activation of the catalyst by adding a co-catalyst, namely an alkyl-aluminum compound (trimethylaluminum TMA, triethylaluminum TEA). There are indications that upon alkylation the Ti cations assume a lower oxidation state (Ti^{3+} or Ti^{2+}), formally according to the equation:[14]

$$TiCl_4 + Al-R_3 \rightarrow R-TiCl_3 + AlClR_2 \rightarrow TiCl_3 + AlClR_2 + R\cdot,$$

where $R = CH_3$, C_2H_5.

However, there has not been direct experimental evidence that supports the formation of radicals in the course of this reaction. Maksimov *et al.*[15] reported in 1974 the presence of an ESR signal at $g = 2.0$ without a discussion of the spectra. However, it is very unlikely that these signals were due to methyl or ethyl radicals, because of the lifetime of these species at room temperature where the spectra were taken. Other investigations are based on scavenger studies, which are problematic because the scavenger molecule can influence the chemistry of the process.[16] Those studies led researchers, however, to assume that the radicals are formed when TMA is used, while for TEA it has been concluded, that the reaction proceeds via disproportionation according to

$$2TiCl_4 + 2Al(C_2H_5)_3 \rightarrow 2TiCl_3 + 2AlCl(C_2H_5)_2 + C_2H_4 + C_2H_6$$

[a]Author to whom correspondence should be addressed. Electronic mail: risse@fhi-berlin.mpg.de. Tel. ++49-30-8413-4218. Fax ++49-30-8413-4316.

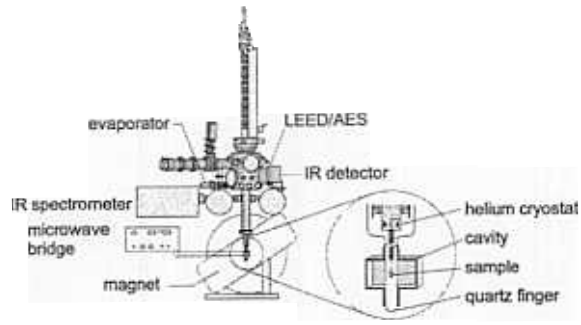

FIG. 1. Schematic representation of the experimental setup.

and not via actual radical formation.[16,17]

In general, it must be stated that in spite of a huge number of studies including those already using surface sensitive techniques, there is a number of open questions that need to be addressed.

In the present study we report results gained on model systems, the preparation of which are based on the work of Somorjai and co-workers.[1,18] For the first time we apply *in situ* ESR spectroscopy[19,20] on such systems in ultrahigh vacuum, and report the direct observation of ethyl radicals. A preliminary account of this particular aspect has been recently published.[21] Furthermore, by combining ESR with FTIR and LEED/Auger measurements we studied the anchoring process of $TiCl_4$ on the $MgCl_2$. It is shown in agreement with the literature that defects play a very important role and we can identify particularly active defects via ESR.

Also, the polymerization of ethylene has been followed at elevated pressures using *in situ* FTIR spectroscopy and it is shown that the resulting polymer shows a certain degree of crystallinity associated with the growth of the polymer film on the modified support surface.

II. EXPERIMENT

The experiments have been performed in an ultrahigh vacuum apparatus (base pressure 2×10^{-10} mbar) shown schematically in Fig. 1. It consists of a preparation stage at the top, which allows for studying the order and the chemical composition of the sample using a LEED/Auger system as well as thermal desorption and residual gas analysis with a quadrupole mass spectrometer. The chamber is pumped with a stack of an ion-getter, a turbo-molecular and a titanium sublimation pump. Also, all necessary materials namely $MgCl_2$, $TiCl_4$, TMA, TEA, and ethylene can be dosed to the surface (see below). The Pd(111) single crystal serving as the substrate for the catalyst preparation is mounted at the end of a helium cryostat which is built into a long travel manipulator and allows a cooling of the sample down to 40 K. With the manipulator, the sample can be transferred to an intermediate position to perform IRAS measurements. We use a FTIR spectrometer from BIO-RAD type FTS-40 VM. The spectrometer is evacuated by a rotary pump to avoid absorption by CO_2 and water. During the measurement, dried nitrogen flows through the spectrometer serving as a gas cushion for the movable mirror of the Michelson interferometer. During operation the pressure ranges in the 10^{-1} mbar regime. The coupling to the vacuum chamber is realized via two KBr windows. The reflected infrared radiation is measured by a mercury–cadmium–telluride (MCT) detector, which is liquid nitrogen cooled. The position of the spectrometer can be mechanically adjusted.

From the IRAS intermediate position the sample may be moved into the ESR stage after passing a metal-glass connection. This ends in a quartz tube (Suprasil) which sits in the bore of an ESR cavity (type TE_{102} from Bruker). The cavity is part of a Bruker EMX spectrometer equipped with a Varian 12-inch high-current electromagnet (V-3603), which has been positioned at an inclination angle of the yoke which allows a shorter z-travel into the measurement position. The magnet can be moved in and out of the measurement position on rails to allow adjustment of sample and cavity. For ESR measurements radiation in the X-band ranging between 9–10 GHz is used. The correspondent wavelengths are around 3 cm. At this wavelength the magnet has to deliver a field strength of 3.4 kG (340 mT) to yield resonance for an electron spin with a g-value of the free electron ($g=2.0023$). The incident microwave power used in the experiments was chosen such that saturation effects are avoided.

The cut and polished Pd(111) sample could be heated up to 1000 °C and its temperature was controlled by a type K thermocouple. It was cleaned by sputter (Ar ions at 1 keV)-anneal (1080 K for 5–10 min) cycles. The sample is mounted on tungsten rods and held by a 0.3 mm tungsten wire loop sitting in slits on three sites of the crystal which allows direct heating. The tungsten rods are connected to a sapphire block which is attached to a copper block. Due to the electrical isolation of the sample, which is realized by squeezing the tungsten rods into a sapphire block mounted to the cryostat, the sample could also be heated by electron impact.

$MgCl_2$ was evaporated as molecular $MgCl_2$ from a Knudsen cell mounted inside the preparation chamber. During evaporation, the Pd(111) single crystal was heated to 700 K and dosed out of the Knudsen cell for 30–60 min. The temperature of the cell was typically 810 K. After this initial evaporation, the Pd(111) substrate was cooled to 610 K and then exposed to $MgCl_2$ vapor for several hours (typically 4–5 hours). During this procedure, we observed an increase of the background pressure to the 10^{-8} mbar range due to hydrogen evanescence from the $MgCl_2$ evaporation material. By prolonged pumping the pressure was brought back to the base pressure range. In order to increase the sensitivity of the ESR measurements, both sides of the Pd(111) crystal have been prepared in this way.

For various steps in the preparation of the model catalyst, the $MgCl_2$ films, whose order and composition was deduced by LEED/Auger, could be bombarded with electrons or ions.

III. RESULTS AND DISCUSSION

A. Preparation of the $MgCl_2/TiCl_4$ model catalyst

Figure 2 shows a series of LEED patterns following the preparation of the $MgCl_2$ film. Figure 2(a) shows the hexago-

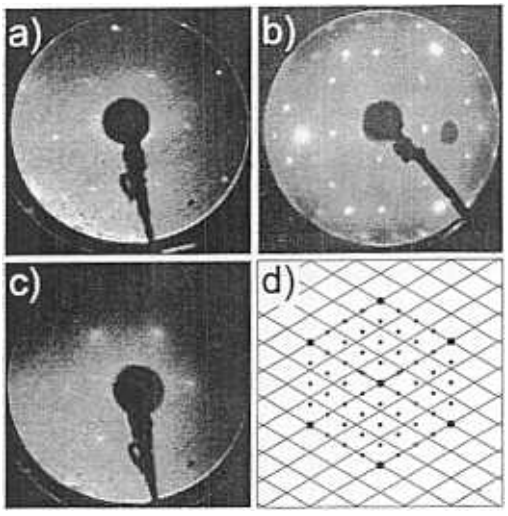

FIG. 2. LEED pattern as observed during preparation of a $MgCl_2$ film. (a) Pd(111), (b) 1 ML $MgCl_2$(001)/Pd(111), (c) multilayer $MgCl_2$(001)/Pd(111), (d) schematic real-space representation of *b*; spots represent the underlying Pd lattice.

nal pattern of the Pd(111) surface after five days of preparation by sputter-anneal cycles. Sulfur and carbon were reduced by this procedure to a level where they could no longer be detected with Auger spectroscopy. As described in the previous section, $MgCl_2$ films are evaporated in two steps. First, at a nominal coverage of a monolayer of $MgCl_2$ a (4×4) LEED pattern is recorded as shown in Fig. 2(b). This structure has been reported before by Fairbrother *et al.*[18,22] as an epitaxial monolayer, where according to the lattice constants of Pd(111) and $MgCl_2$(001), three unit cells of $MgCl_2$(001) fit onto four Pd(111) cells. A schematic representation of this situation is shown in Fig. 2(d). Upon further increase of the $MgCl_2$ thickness the orientation of the $MgCl_2$ does not change, but a regular hexagonal structure representing the $MgCl_2$(001) surface is visible. From a quantitative evaluation of the Pd signal attenuation as a function of thickness, the film thickness is estimated to be 6–12 layers of $MgCl_2$. Figure 3 shows a schematic diagram summarizing the structures observed. It is clear, that even though the surface is polar, the system is stable due to the $MgCl_2$ structure, which is a case B according to the Tasker rules.[23]

It is important to study whether the prepared $MgCl_2$ film exhibits pinholes. This can be done via adsorption of CO and subsequent TDS studies. The only signals observed are in the region of 70 K, which is compatible with desorption from the $MgCl_2$ film. There are no signals in the range where CO desorbs from Pd(111), i.e., near 540 K.[24] On a $MgCl_2$ surface

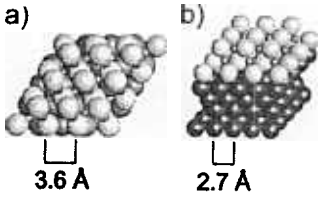

FIG. 3. Schematic representation of a chlorine terminated $MgCl_2$(001) film on Pd(111): (a) top view; (b) perspective view.

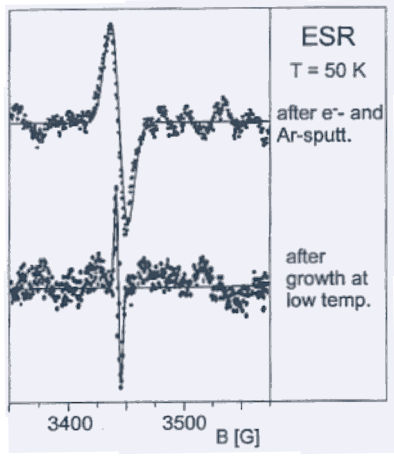

FIG. 4. ESR spectra of color centers in a $MgCl_2$ film for two different preparation conditions. Top: An initially well ordered film after bombardment with electrons and argon ions; bottom: film grown at reduced temperature.

prepared in this way, $TiCl_4$ does not adsorb at room temperature. $TiCl_4$ can of course, be condensed onto the surface at low temperature, but by elevating the temperature, all $TiCl_4$ desorbs well below room temperature.[25]

Magni and Somorjai in their pioneering work already realized that it is necessary to produce defects in the film to bind the $TiCl_4$ precursor.[1,12,26] The idea really goes back even further,[27] however. Early on it was noted that the uncoordinated edge and corner sites on a $MgCl_2$ crystallite bind $TiCl_4$.[3,7,28] This was also corroborated by recent model calculations.[10,29]

There are several ways to produce defect containing surfaces: One way is to keep the Pd(111) surface temperature low, so that the mobility of the $MgCl_2$ is too low to produce a fully epitaxial film. However, the problem here is, that such films often contain pinholes, which change the reactivity of the system. Therefore, it has been considered to first create a fully epitaxial film and then produce defects by either electron or ion bombardment.[1,12,26] Figure 4 compares the ESR spectra for the two cases, namely defects created at lower growth temperature (bottom) and after a sequential bombardment with electrons and argon ions. Obviously, part of the created defects are ESR active, while others may not be, and they are, of course, not represented in the spectra. The question is, which defects are represented in the spectra? It is known, that upon irradiation of alkali and alkali-earth halogenides with x-ray and gamma-radiation or electrons color centers (F-centers) with unpaired electrons are formed.[30–32] If these centers are created in large amounts, they can be stabilized by the formation of metal clusters. Such metal clusters show conduction electron-spin resonance (CESR).[31] For systems with an even number of conduction electrons—such as magnesium—color centers and CESR can experimentally be differentiated by considering the temperature dependence of the signals. While color centers show a Curie-type temperature behavior ($\sim 1/T$), CESR signals are rather weak and do not exhibit a pronounced temperature dependence in the range of temperatures used here, as the susceptibility is equal to the temperature-independent Pauli-

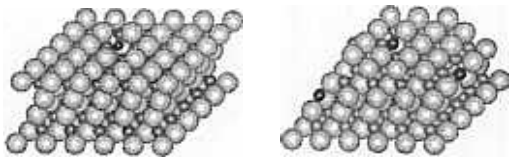

FIG. 5. Sketch of different environments of surface color centers on a smooth and a highly defective surface.

susceptibility.[30–33] Furthermore, the linewidths of these clusters are very large as long as quantum size effects are not important. Let us first consider the nonepitaxial film. Both, position of the maximum in the lower trace, as well as the temperature dependence, which is Curie-type, favor the formation of color centers. For a more detailed assignment we resort to the work of Giamello and co-workers on color centers in MgO.[32] The position of the present signal is close to the one observed for color centers in the bulk, i.e., a missing Cl ion replaced by an electron. The hyperfine splitting due to the presence of neighboring Mg ions is not visible above noise, which is expected because of the low natural abundance of the ^{25}Mg isotope (10.1%, $I=5/2$).

If we grow an epitaxial film as done for the upper trace, there is no detectable ESR signal before further treatment of the film and the film comprises a sharp LEED pattern with low background intensity. Bombardment of the film with electrons or argon ions does disturb the structure as judged by the background of the LEED picture, as well as Auger spectroscopy, which shows a loss of chlorine especially for the electron-induced process. However, none of these processes is sufficient to create an ESR active defect. Subsequent argon ion bombardment (150 eV, 1 μA/cm^2, 3 min.) of a sample initially exposed to electrons does produce an ESR signal as shown in Fig. 4. As compared to the spectra of the defects created by growth at lower temperatures, the signal is shifted to higher g-values. Additionally, the linewidth increases from 4 to 14 G. This might be explained by the creation of color centers on the rough surface exposing different low coordinated sites which will have slightly different g-values as compared to the color center on the (001) terrace. A schematic view of the situation is shown in Fig. 5.

$TiCl_4$ has a high enough vapor pressure to dose the molecule from the gas phase. Adsorbing $TiCl_4$ under electron bombardment on the samples where the $MgCl_2$ film was grown nonepitaxially quenches the signal by 40%. We take this as a clear indication that part of the defects are localized on the surface of the magnesium-chloride film, while most of the defects detected in this case are bulk defects not influenced by the adsorbed $TiCl_4$.

The question is now, what is the chemical state of the Ti bound to the $MgCl_2$ surface? Somorjai and co-workers[1,12,26] showed by XPS measurements that Ti exists on the surface as Ti^{2+} and Ti^{4+}, and there was no Ti^{3+} detectable. ESR should allow us to test the result, because Ti^{3+} as a d^1-system should be ESR active if in a monomeric form. Two distinctly different ESR spectra due to Ti^{3+} centers have been observed as shown in Fig. 6. In the first case a relatively sharp signal with a peak-to-peak width of 14 G is observed at $g=1.96$, if a surface is used which does not exhibit paramagnetic defects. This signal appears after exposing the surface to $TiCl_4$ in the presence of electrons and subsequent electron bombardment. It should be noted that systems not exposed to additional electrons after $TiCl_4$ adsorption do not exhibit this signal. The signal shows Curie-type temperature behavior. Upon aluminum-alkyl exposure the signal loses intensity. Depending on the preparation, the reduction of the intensity ranges from 10 to 60%, indicating that the amount of surface species varies for the different preparations.

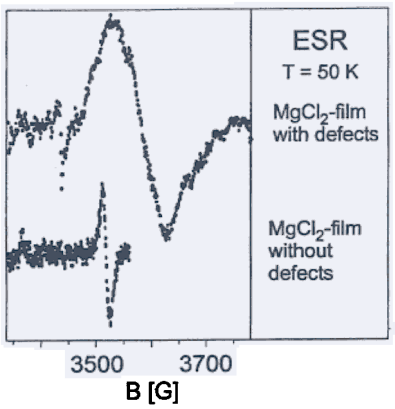

FIG. 6. ESR spectra of Ti^{3+} centers at 50 K after deposition of $TiCl_4$ under prolonged electron bombardment on a defected $MgCl_2$ film (top) and a defect-free $MgCl_2$ film (bottom).

The other signal has been observed after adsorption of $TiCl_4$ during electron bombardment on a surface showing paramagnetic defects if the deposit is treated subsequently either with electrons or with argon ions. As shown in Fig. 6 the signal differs strongly from the one in the above-mentioned in the sense that it is located around $g=1.93$ and has a peak-to-peak width from 50 to 90 G, depending on the preparation. As compared to the sharp signal at $g=1.96$, the intensity of this broad signal is about an order of magnitude larger.

The g-value found is situated among values reported for $TiCl_3$ in octahedral ($g=1.94$) and tetrahedral ($g=1.97$) environments.[34] These values have been measured for Ziegler–Natta catalysts, but also in those cases there is no clear indication for a correlation with the catalyst activity. While the signal observed on the less defected surface is close to the value observed for tetrahedral environments, the signal of the surface showing paramagnetic defects is centered at the value for octahedral environments. Comparing the linewidth of the signals measured here with the ones in the literature, the general trend of the signal at $g=1.94$ being broader than the ones at $g=1.96$ holds true also for these measurements; however, the linewidth of the resonance at $g=1.93$ is considerably broadened as compared to literature. Considering the stronger disorder of these systems, it is more likely that isolated Ti^{3+} centers are formed in this case which may comprise different local environments and thus showing a larger linewidth.

However, there is no indication that the presence of the observed signals correlates with the polymerization efficiency of the catalyst. In fact, systems which exhibit these signals are less effective catalysts and in some cases do not

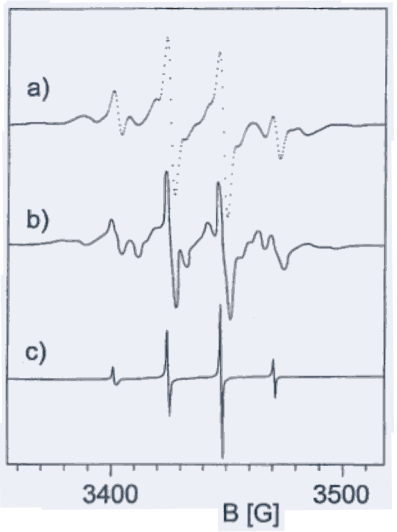

FIG. 7. ESR spectra of the model catalyst (a) after adsorption of $AlMe_3$ at 50 K. (b) ESR spectrum of ethyl radicals at 77 K (Ref. 38). (c) ESR spectrum of methyl radicals at 77 K (Ref. 37).

even polymerize ethylene under the chosen conditions. On the contrary, systems without ESR signals correlated to Ti^{3+} species are found to be catalytically active. The lack of an ESR signal corresponding to Ti^{3+} ions in cases, where no additional argon or electron bombardment has been applied, cannot be interpreted as a clear indication for the absence of Ti^{3+} at the surfaces. In the literature there are discussions that small spin-lattice relaxation times, dipole coupling, and super exchange may only leave a very small fraction of Ti^{3+} detectable due to increase in linewidth.[35]

B. Activation of the catalyst

The $TiCl_4/MgCl_2$ system is, as it is called in Ziegler–Natta catalysis, activated by exposing it to the co-catalyst, i.e., an aluminum-alkyl compound. We have used trimethylaluminum (TMA) and triethylaluminum (TEA) for activation. The compounds have been dosed from the gas phase either at room temperature for a prolonged time or much shorter at 40 K surface temperature. Typically, 3400 L of TMA or TEA were exposed. The infrared spectrum of the condensed film showed the typical FTIR spectrum known from condensed and matrix isolated species.[36] There are bands that can be assigned to dimeric aluminum-alkyl species.

Figure 7 shows ESR spectra after reaction of the TMA with the $TiCl_4/MgCl_2$ system.[21] A typical low coverage of $TiCl_4$ leads to the spectra shown in the upper trace. Increasing the amount of $TiCl_4$ on the surface by a factor of three increases the intensity of the ESR spectrum by a factor of 1.7, which indicates that the amount of surface titanium centers increases with total amount of titanium on the surface. This can be understood by means of an islandlike growth mode of the $TiCl_4$ on the surface. The spectrum is free of any Ti^{3+} signal. This is in accordance with the observation in the literature, namely the formation of mainly Ti^{2+} species due to the reduction with aluminum alkyls.[14] Although it might be thought that methyl radicals are the most natural products in the reduction of a mixed titanium-chlorine-methyl species, a comparison of the line shape of the observed spectra with spectra of methyl radicals (shown at the bottom of Fig. 7) taken from the literature[37] clearly shows that the species present here are not methyl radicals. Whereas the ESR spectrum of a methyl radical is a quartet of lines, the spectrum observed here, though dominated by a quartet structure, shows a couple of additional lines pointing to additional interactions of the unpaired electron. By comparing the line shape to other alkyl radicals, it turned out that the present spectrum can be attributed to ethyl radicals. Figure 7 shows for comparison ethyl radicals created in an ethylchloride matrix generated by photolysis.[38] The line shape of the ethyl radicals can be understood when assuming that the protons of the methyl group adjacent to the spin containing methylene group, which cause superhyperfine interaction with the unpaired electron, are magnetically equivalent due to a fast rotation of the methyl group along the C–C bond. The two protons of the methylene group, however, give rise to anisotropic superhyperfine interactions because of the adsorption of the molecule on the surface hinders a rotation of the molecule in space. Assuming the anisotropic interaction to be axially symmetric allows a good description of the observed line shape as shown by Shiga *et al.*[37]

There are two key questions, that have to be answered:

1. How have the C_2H_5 radicals been created?
2. Have the radicals been created at the TMA/$TiCl_4$–$MgCl_2$ interface or in the TMA activating materials?

The second question can be answered by studying the amount of radicals formed as a function of the amount of $TiCl_4$ at the interface and as a function of exposed TMA. As a function of $TiCl_4$ the ESR intensity increases for a low $TiCl_4$ concentration regime, but it shows a clear saturation behavior when plotted versus the amount of TMA adsorbed. Both observations are compatible with a radical creation process happening at the TMA/$TiCl_4$–$MgCl_2$ interface, where an alkylation of the $TiCl_4$ by ligand exchange is supposed to happen. Assuming this ligand exchange to occur, the primary radical that can be created is a methyl radical. For this radical there are several possibilities for consecutive reactions given the size and high mobility, even at low temperature, in the solid state.[39]

The most likely reaction yielding ethyl radical is

$$CH_3\cdot + Al(CH_3)_3 \rightarrow H_3C-H_2C\cdot + AlH(CH_3)_2.$$

Even though such a reaction has not been investigated so far, it can be crudely estimated that it is energetically possible. Above 50 K the intensity of the ethyl radicals is attenuated irreversibly and decreases below the detection limit above 80 K. This can be explained by assuming the ethyl radicals to diffuse and recombine at these temperatures, as has been observed for methyl radicals above 45 K[40] and NO_2 radicals on an oxide surface above 75 K.[20]

After unreacted TMA has all been desorbed, still carbon, due to the successful alkylation of the $TiCl_4$, is found on the surface. It is, however, important to note that after removing the reacted $TiCl_x$ moieties from the surface, e.g., by soft

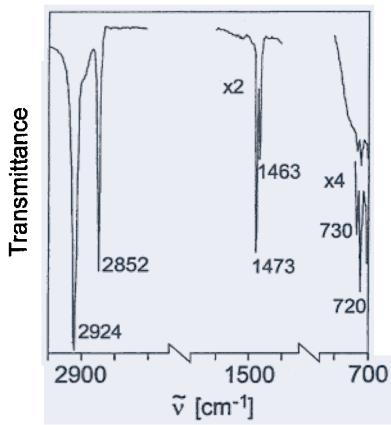

FIG. 8. IR spectrum of the polyethylene film grown on the model catalyst.

argon sputtering, and redosing with TMA, new C_2H_5 radicals can be created.

An interesting observation is made if TEA is used instead of TMA. Even though the catalyst can be activated in a similar way as for TMA, radicals have never been observed. This is in line with expectations because here a disproportionation has been proposed according to

$$AlEt_3 + TiCl_4 \rightarrow AlEt_2Cl + TiCl_3Et,$$

$$2TiCl_3Et \rightarrow 2TiCl_3 + C_2H_4 + C_2H_6.$$

Because ethyl radicals have been observed in the preceding experiment, which also suggests that these radicals are stable at a given temperature, the initial formation of ethyl radicals would undoubtedly lead to observation of the radicals. The absence of an ESR spectrum therefore strongly supports a disproportionation reaction in accordance to interpretation in the literature from indirect evidence.[16,17]

C. Polymerization of ethylene

The model catalyst prepared according to the procedure presented previously was exposed at room temperature to 15 to 150 mbar ethylene. The gas was introduced through the gas-dosing system into the IR chamber. Figure 8 shows the IR spectrum of the generated polyethylene. Characteristic are the stretching modes at 2852/2924 cm^{-1}, the doublets of the deformation modes at 1473/1463 cm^{-1}, and the rocking modes at 730/720 cm^{-1} (see Table I). In comparison with the literature the observed frequencies of the stretching modes are situated at the higher end for dominating *trans*-configurations. This was taken as an indication that the polymer chains have long range order in *trans*-configurations but also contain some gauche defects. Similar results were also obtained in other work. Polyethylene formed via diazomethane reaction on Au(111) films showed similar behavior.[41] Also, n-$C_{44}H_{90}$ adsorbed on Au surfaces yielded analogous results. Here the authors found gauche defects only in the second layer, while the first represented a flat lying chain.[42]

Some indications for the existence of partially crystalline polyethylene can be derived from an analysis of the deformation modes. While a broad resonance at 1468 cm^{-1} points to rather poor order, a sharp doublet indicates crystalline polyethylene.[43,44] The doublet is caused by a Davidov splitting due to the presence of two polyethylene chains in the unit cell.[42,45] In the present case the relative small half-width is a good hint towards a rather well developed crystallinity of the produced polyethylene.[42,45] Typical for crystalline polyethylene is also the split rocking mode at 730/720 cm^{-1}.[43] It is remarkable that vibrations in the range between 720 and 1300 cm^{-1} are completely missing. This observation can be used to estimate a lower limit to the chain length. From a comparison with alkane chains of increasing length it has been deduced that for chain lengths greater than 20 units, the linewidth becomes so large that they cannot be observed. This chain length of 20 units is then the lowest limit in our case.[41,46]

The course of the reaction has been studied by evaluating the IR band at 2852 cm^{-1}, which is the one least influenced by the presence of gaseous ethylene. The polymerization has been followed for 12 to 150 h.

Two different kinds of behavior have been observed. Typical results are given in Fig. 9. The determining factor is here the degree of disorder in the surface of the model catalyst. While a catalyst with a high degree of disorder shows a monotonous increase of the polyethylene amount with time, catalysts prepared on a smooth and less defected surface show a self-terminating reaction after approximately 50 h leading to considerably less thick film as compared to the former case. This can be explained in a straightforward way by considering that on a smooth surface a rather smooth

TABLE I. Comparison of IR frequencies between the model catalyst and data from literature as well as the assignment of the frequencies taken from the literature.

		Assignment
2924	2922–2926 without 2915–2920	CH_2 asymmetr. stretching mode d^-: crystalline PE with gauche-defect[a]
2852	2852–2856 without 2846–2850	CH_2 symmetr. stretching mode d^+: crystalline PE with gauche-defect[b]
1473	1470–1473	CH_2 deformation mode orthorom. PE a-axis[c]
1463	1463	CH_2 deformation mode orthorom. PE b-axis[c]
730	730–731	CH_2 rocking mode orthorom. PE a-axis[d]
720	720	CH_2 rocking mode orthorom. PE b-axis[e]

[a]References 41, 42, and 49.
[b]References 41, 42, 49, and 50.
[c]References 44 and 49–51.
[d]References 43 and 52.
[e]References 43, 52, and 53.

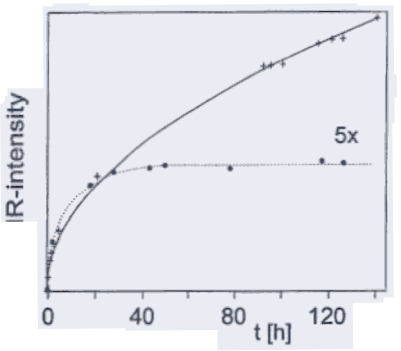

FIG. 9. Kinetics of the polymerization reaction as measured by IR absorption at 2852 cm^{-1}. The kinetics observed on a rough catalyst is represented by the full line, the kinetics observed on a catalyst with a smooth and less defected surface behaves as indicated by the dotted line.

polymer film forms, which in a relatively short time becomes impermeable for ethylene from the gas phase so that the reaction is self-limiting. In the other case, the growing film possibly has a sufficient number of pores so that the monomer can continue to reach the catalyst and the reaction keeps going. This assumes that the polymerization reaction takes place at the interface of the polymer and the magnesium chloride support, which has been corroborated experimentally.[47] The latter behavior can be modeled by assuming that the monomer molecules are transported by diffusion to the interface. The amount of polymer n_e increases with reaction time t according to

$$n_e = \delta\sqrt{t},$$

where the constant δ is a function of the diffusion coefficient, the surface area, the molar volume of the polymer, and the concentration at infinite time t.

Therefore, we expect that the IR intensity increases as $\sqrt{t}$. With $\delta = 4.6 \cdot 10^{-2}$ mol $s^{-1/2}$ the fit given in Fig. 9 has been obtained.

The polymer film shows a clear ESR signal. It is located near $g = 2.002$ and can be assigned to Ti^{3+} centers with organic environment.[48] The signal varies in intensity and width considerably from preparation to preparation, but there is no correlation with activity. It is very likely that the signal is due to Ti^{3+} compounds interacting with the polymer that gives rise to the signal but a unique assignment cannot be given.

IV. SUMMARY AND CONCLUSIONS

A model catalyst to study Ziegler–Natta catalysis of ethylene polymerization has been prepared and characterized at various steps of the preparation procedure. We have applied a unique combination of ESR and FTIR together with LEED/Auger to assign the creation of defects during the preparation and the creation of ethyl radicals during activation. In fact, this study provides first direct evidence for alkyl radicals being involved in the preparation of the Ziegler–Natta catalyst. We do observe Ti^{3+} species, but their occurrence cannot be directly connected with the reactivity of the system.

Polymerization has been observed and a partially crystalline *trans*-polyethylene containing gauche defect has been found. The course of the reaction depends on the morphology of the substrate, leading to self-limited reactions in the case of smooth surfaces.

ACKNOWLEDGMENTS

The authors are grateful to a number of agencies who funded the work: Deutsche Forschungsgemeinschaft, Ministerium für Wissenschaft und Forschung Nordrhein-Westfalen, Fonds der Chemischen Industrie, as well as Max-Planck-Gesellschaft.

[1] E. Magni and G. A. Somorjai, Catal. Lett. **35**, 205 (1995).
[2] K. Ziegler, E. Holtzkamp, H. Martin, and H. Breil, Angew. Chem. **67**, 541 (1955).
[3] P. C. Barbé, G. Cecchin, and L. Noristi, Adv. Polym. Sci. **81**, 1 (1987).
[4] W. Kaminsky and M. Arndt, in *Handbook of Heterogeneous Catalysis*, edited by G. Ertl, H. Knözinger, and J. Weitkamp (Wiley-VCH, Weinheim, 1997), Vol. 5, p. 2405.
[5] G. Natta, J. Polym. Sci. **16**, 143 (1955); G. Natta, P. Pino, and P. Mazzanti, U.S.A. Patent No. 3,715,344 (1954).
[6] *Ziegler Catalysts*, edited by G. Fink, R. Mühlhaupt, and H. H. Brintzinger (Springer, Heidelberg, 1994).
[7] J. J. A. Dusseault and C. C. Hsu, J. Macromol. Sci. Rev. Macromol. Chem. C **33**, 103 (1993).
[8] T. Keii, *Kinetics of Ziegler–Natta Polymerization* (Chapman & Hall, London, 1982); J. Boor, *Ziegler–Natta Catalysts and Polymerization* (Academic, New York, 1979); Y. V. Kissin, *Isospecific Polymerization of Olefins* (Springer, Berlin, 1985); P. Pino and R. Mühlhaupt, Angew. Chem. Int. Ed. Engl. **19**, 857 (1980); H. Sinn and W. Kaminsky, Adv. Organomet. Chem. **18**, 99 (1980); I. Pasquon and U. Giannini, in *Catalytic Olefin Polymerization*, in *Catalysis, Science and Technology*, edited by J. R. Anderson and M. Boudart (Springer, Berlin, 1984), Vol. 6, p. 65; *Coordination Polymerization*, edited by J. C. W. Chien (Academic, New York, 1975); *Transition Metal Catalyzed Polymerizations*, edited by R. P. Quirk (Harwood, New York, 1985), Vol. 4, Parts A and B; *Transition Metal Catalyzed Polymerization: Ziegler–Natta and Metathesis Polymerizations*, edited by R. P. Quirk (Cambridge University Press, Cambridge, 1988); *Studies in Surface Science and Catalysis*, edited by T. Keii and K. Soga (Elsevier-Kodansha, Tokyo, 1986), Vol. 25; *History of Polyolefins*, edited by R. B. Seymour (Reidel, Dordrecht, 1985); *Transition Metals and Organometallics as Catalysts for Olefin Polymerization*, edited by W. Kaminsky and H. Sinn (Springer, Berlin, 1988); *Polypropylene and Other Polyolefins*, edited by S. V. D. Veen (Elsevier, Amsterdam, 1990).
[9] M. R. Mason, J. Am. Chem. Soc. **115**, 4971 (1993); C. J. Harlan, M. R. Mason, and A. R. Barron, Organometallics **13**, 2957 (1994); H. Sinn, Macromol. Symp. **97**, 27 (1995).
[10] M. Boero, M. Parrinello, H. Weiss, and S. Hüfter, J. Phys. Chem. A **105**, 5096 (2001).
[11] I. Hemmerich, F. Rohr, O. Seiferth, B. Dillmann, and H.-J. Freund, Z. Phys. Chem. (Munich) **202**, 31 (1997); P. C. Thüne, J. Loos, P. J. Lemstra, and H. Niemantsverdriet, J. Catal. **183**, 1 (1999).
[12] E. Magni and G. A. Somorjai, Appl. Surf. Sci. **89**, 187 (1995); E. Magni and G. A. Somorjai, Surf. Sci. **345**, 1 (1996); E. Magni and G. A. Somorjai, J. Phys. Chem. **100**, 14786 (1996); T. A. Koránvi, E. Magni, and G. A. Somorjai, Top. Catal. **7**, 179 (1999).
[13] S. H. Kim and G. A. Somorjai, Appl. Surf. Sci. **161**, 333 (2000).
[14] E. Magni and G. A. Somorjai, Surf. Sci. **377**, 824 (1997); S. H. Kim and G. A. Somorjai, J. Phys. Chem. B **105**, 3922 (2001).
[15] N. G. Maksimov, E. G. Kushnareva, V. A. Zakharov, V. F. Anufrienko, Y. Zhdan, and I. Ermakov, Kinet. Katal. **15**, 738 (1974).
[16] U. Thewalt, in *Gmelins Handbuch der Anorganischen Chemie* (Springer, Heidelberg, 1977), Vol. 40, Teil 1; H. de Vries, Recl. Trav. Chim. Pays-Bas. **80**, 866 (1961).
[17] C. Beermann and H. Bestian, Angew. Chem. **71**, 618 (1959); F. S. D'yachowvskii, N. E. Khrushch, and A. E. Shilov, Kinet. Katal. **9**, 831 (1968).
[18] D. H. Fairbrother, J. G. Roberts, S. Rizzi, and G. A. Somorjai, Langmuir **13**, 2090 (1997).
[19] U. J. Katter, H. Schlienz, M. Beckendorf, and H.-J. Freund, Ber. Bunsenges. Phys. Chem. **97**, 340 (1993).

[20] H. Schlienz, M. Beckendorf, U. J. Katter, T. Risse, and H.-J. Freund, Phys. Rev. Lett. **74**, 761 (1995).
[21] T. Risse, J. Schmidt, H. Hamann, and H.-J. Freund, Angew. Chem. (unpublished).
[22] D. H. Fairbrother, J. G. Roberts, and G. A. Somorjai, Surf. Sci. **399**, 109 (1998).
[23] P. W. Tasker, Adv. Ceram. **10**, 176 (1984).
[24] X. Guo, A. Hoffman, and J. T. Yates, Jr., J. Chem. Phys. **90**, 5787 (1989).
[25] J. Schmidt, Ph.D. thesis, Ruhr-Universität Bochum, 2001.
[26] E. Magni and G. A. Somorjai, Surf. Sci. Lett. **341**, L1078 (1995).
[27] P. Galli, P. C. Barbé, G. Guidetti, R. Zannetti, A. Marigo, M. Bergozza, and A. Fichera, Eur. Polym. J. **19**, 19 (1983); R. Gerbasi, A. Marigo, A. Martorana, R. Zannetti, G. Guidetti, and G. Baruzzi, *ibid.* **20**, 967 (1984).
[28] P. Corradini and G. Guerra, Prog. Polym. Sci. **16**, 239 (1991).
[29] C. Martinsky, C. Minot, and J. M. Ricart, Surf. Sci. **490**, 237 (2001).
[30] S. Kinno and R. Onaka, J. Phys. Soc. Jpn. **52**, 267 (1983).
[31] G. C. Fryburg and R. J. Lad, Surf. Sci. **48**, 353 (1975); H. W. den Hartog, P. Mollema, and A. Schaafsma, Phys. Status Solidi B **55**, 721 (1973).
[32] E. Giamello, D. Murphy, L. Ravera, S. Coluccia, and A. Zecchina, J. Chem. Soc., Faraday Trans. **90**, 3167 (1994).
[33] S. Sako and K. Kimura, Surf. Sci. **156**, 511 (1985); J.-L. Millet and J.-P. Borel, *ibid.* **106**, 403 (1981).
[34] J. Peyroche, Y. Girard, R. Laputte, and A. Guyot, Makromol. Chem. **129**, 215 (1969); K. Soga and M. Terano, *ibid.* **182**, 2439 (1981); V. A. Zakharov, S. I. Makhtarulin, V. A. Poluboyraov, and V. F. Anufrienko, *ibid.* **185**, 1781 (1984).
[35] J. C. W. Chien and J. C. Wu, J. Polym. Sci., Polym. Chem. Ed. **20**, 2461 (1982); , *ibid.* **20**, 2461 (1982); H. Fuhrmann and W. Herrmann, Macromol. Chem. Phys. **195**, 3509 (1994).
[36] S. Kvisle and E. Rytter, Spectrochim. Acta, Part A **40**, 939 (1984).
[37] T. Shita, H. Yamaohu, and A. Lund, Z. Naturforsch. A **29A**, 653 (1974).
[38] P. B. Ayscough and C. Thomson, Trans. Faraday Soc. **58**, 1477 (1962).
[39] R. L. Morehouse, J. J. Christiansen, and W. Gordy, J. Chem. Phys. **45**, 1751 (1966).
[40] K. Toriyama, M. Iwasaki, and K. Nunome, J. Chem. Phys. **71**, 1698 (1979).
[41] K. Seshadri, S. V. Atre, Y.-T. Tao, M.-T. Lee, and D. L. Allara, J. Am. Chem. Soc. **119**, 4698 (1997).
[42] M. Yamamoto, Y. Sakurai, Y. Hosoi, H. Ishii, K. Kajikawa, Y. Ouchi, and K. Seki, J. Phys. Chem. B **104**, 7363 (2000).
[43] R. G. Snyder, J. Mol. Spectrosc. **7**, 116 (1961).
[44] M. Tasumi and T. Shimanouchi, J. Chem. Phys. **43**, 1245 (1965); M. C. Tobin and M. J. Carrano, *ibid.* **25**, 1044 (1956).
[45] S. Krimm, C. Y. Liang, and G. B. B. Sutherland, J. Chem. Phys. **25**, 549 (1956).
[46] R. G. Snyder, J. Chem. Soc., Faraday Trans. **88**, 1823 (1992); J. R. Nielsen and R. F. Holland, J. Mol. Spectrosc. **6**, 394 (1961).
[47] S. H. Kim and G. A. Somorjai, Catal. Lett. **68**, 7 (2000).
[48] H. J. M. Bartelink, H. Bos, J. Smidt, C. H. Vrinssen, and E. H. Adema, Recl. Trav. Chim. Pays-Bas. **81**, 225 (1962); S. A. Sergeev, V. A. Poluboyarov, V. A. Zakharov, V. F. Anufrienko, and G. D. Bukatov, Makromol. Chem. **186**, 243 (1985).
[49] P. Zielinski and I. G. Dalla Lana, J. Catal. **30**, 2324 (1992).
[50] D. Scarano, G. Spoto, S. Bordiga, L. Carnelli, G. Ricchiardi, and A. Zecchina, Langmuir **10**, 3094 (1994).
[51] B. Rebenstorf, J. Mol. Catal. **45**, 263 (1988).
[52] G. Zerbi and G. Gallino, Polymer **30**, 2324 (1989).
[53] R. G. Snyder and J. H. Schachtschneider, Spectrochim. Acta **19**, 85 (1963).